Anomalous Viscosity Decrease of Polycarbonate by Addition of Polystyrene

Takumi Sako[a], Jitsuhiro Date[a], Misaki Hagi[b], Tatsuhiro Hiraoka[b], Shinji Matsuoka[b], and Masayuki Yamaguchi*[a]

a) School of Materials Science, Japan Advanced Institute of Science and Technology

b) Otake R&D Center, Mitsubishi Chemical Corporation

*Correspondence to Masayuki Yamaguchi
Phone: +81-761-51-1621; Fax: +81-761-51-1149
E-mail: m_yama@jaist.ac.jp

Abstract

The shear viscosity of binary blends comprising polycarbonate (PC) and low-molecular-weight polystyrene (L-PS) was examined. It was found that the viscosity of PC significantly decreases by the addition of L-PS. Although the dynamic mechanical properties indicated that L-PS is immiscible with PC, the morphology observation of the extruded strand clarified that shear-induced phase-mixing occurs. Furthermore, the viscosity decrease was found to be pronounced in the high shear stress condition, which is much more obvious than that by the addition of low-molecular-weight PC. Consequently, the addition of L-PS improves the flowability at injection-molding greatly.

Keywords; Viscoelasticity; Capillary flow; Polymer blend

Introduction

Rheological properties of miscible polymer blends have been intensely studied. A negative and/or positive deviation of the zero-shear viscosity from the log additive rule has been discussed based on experimental results.[1)] The rheological properties for miscible polymer blends are, however, still unknown especially near the phase transition because of the poor understanding of the free volume fraction, monomeric friction coefficient, and nematic interaction, i.e., orientation correlation.[2-4)]

In this study, the rheological properties for one of the most important polymer blends in industry, that is, polycarbonate (PC) and PS, were studied. Although the blend system is considered to be immiscible,[5-7)] it was first found that they show flow-induced phase-mixing when the content of low-molecular-weight PS is low. Moreover, phase separation occurs immediately after the cessation of flow. Consequently, the glass transition temperature of the PC phase in the blend, which determines the heat resistance, is the same as that of pure PC. Furthermore, the transparency is not affected by the addition of PS even after the phase separation because of the refractive index matching. Finally, the large decrease in the shear viscosity, especially at high shear rates, leads to an enhanced flowability at injection-molding, which is evaluated by spiral-flow length. This is an attractive property to obtain a large-size product. Although some studies on the viscosity decrease for PC have been carried out by the addition of a third component,[8,9)] the present study is different from them and much more conducive for actual material design.

Experimental

Materials and sample preparation

Two types of commercially available bisphenol A polycarbonate with different molecular weights were employed; the one having a high molecular weight was denoted as PC and the other with a low molecular weight was denoted as L-PC. Furthermore, low-molecular-weight atactic polystyrene (L-PS) was used in this study.

The average molecular weights, glass transition temperature (T_g), and zero-shear viscosity (η_0) for each sample are summarized in Table 1. The number- and weight-average molecular weights were measured by size exclusion chromatography (HLC-8020, Tosoh) with polystyrene standard samples using chloroform as solvent. The T_gs were evaluated by differential scanning calorimetry (DSC8500, Perkin-Elmer) at a heating rate of 10 °C/min. The η_0 values were evaluated at 250 °C by the oscillatory shear measurements using a cone-and-plate rheometer (AR2000ex, TA Instruments).

Table 1 Characteristics of polymers employed

	M_n	M_w	T_g (°C)	η_0 at 250 °C (Pa s)
PC	18,000	45,000	151	2,800
L-PS	25,000	51,000	106	11
L-PC	3,100	7,300	119	2.7

The blends of PC/L-PS and PC/L-PC were prepared by a twin-screw extruder (UTL15TWnano, Technovel) at 260 °C and 50 rpm. The contents of the low-molecular-weight polymers were 5 and 10 wt.% for L-PS, and 10 wt.% for L-PC. After extrusion from a circular die, the strand was cooled in a water bath and cut into a pellet shape by a pelletizer. The pellets were dried at 80 °C for 6 hours under vacuum to remove water.

The pellets were directly used for the capillary extrusion measurements. Compression-molded films were also prepared for dynamic mechanical measurements. After applying a pressure of 10 MPa for 3 min at 250 °C, the sample was cooled at 25 °C by another compression-molding machine with a cooling unit. The same processing history was also applied to pure PC as a reference.

Measurements

The temperature dependence of the tensile storage modulus (*E'*) and loss modulus (*E"*) was measured using a dynamic mechanical analyzer (E-4000, UBM) from 30 to 180 °C. The frequency and the heating rate were 10 Hz and 2 °C/min, respectively. A rectangular specimen, with the size of 20 × 5 × 0.3 mm cut from the film, was employed for the measurement.

The frequency dependence of shear storage modulus (*G'*) and loss modulus (*G"*) in the molten state was measured using a cone-and-plate rheometer (AR2000ex, TA Instrument) within the angular frequency range from 0.1 to 396 s^{-1}. The angle of the cone was 4° and the diameter was 25 mm. The measurements were performed at 230, 250, and 280 °C. The growth curves of the shear viscosity were also obtained by the cone-and-plate rheometer at constant shear rates of 0.1 s^{-1} and 2.3 s^{-1} at 250 °C.

The pressure-driven flow behavior was evaluated using a capillary rheometer (140SAS, Yasuda Seiki Seisakusyo). Circular dies with various ratios of length (*L*) and diameter (*D*) were employed. The entrance angle of the dies was 180°. The temperature in the barrel and die was maintained at 230, 250, and 280 °C. The measurements were performed at 6 different shear rates from 36 to 1000 s^{-1}. Furthermore, the flowability

was evaluated by the spiral-flow length at injection-molding (SE100DU, Sumitomo Heavy Industries). The barrel and mold temperatures were controlled at 300 and 80 °C, respectively. The injection pressure was 40 MPa and the injection speed was 100 mm/s.

The distribution of the blend composition in the extruded strand was investigated in the radial direction by an FT-IR microscope (Spotlight 200, Perkin-Elmer). Thin test pieces with a thickness of 10 μm, which were cut from the center of a strand along the flow direction using a microtome (RX-860, Yamato Koki), were employed for the evaluation. The measurements were performed by transmission mode at various points of the cross-section from the surface to the center. The spectrum at the surface of a strand was also measured directly by the attenuated total reflectance (ATR) mode using KRS-5 as an ATR crystal.

The morphology of the extruded strand was observed by a scanning electron microscope (SEM; E-4100, Hitachi). The same test pieces for the IR measurement were also used for the SEM observation. Prior to the SEM observation, the sample was etched by cyclohexane to remove the L-PS phase and coated by platinum-palladium using an ion spatter machine to avoid charge-up.

Results and Discussion

Figure 1 shows the temperature dependence of E' and E'' for the compression-molded films of PC, PC/L-PS (5%), PC/L-PS (10%), and PC/L-PC (10%). The E'' curves for the PC/L-PS blends exhibited distinct double peaks, which were ascribed to the glass-to-rubber transition of both polymers. Correspondingly, the E' showed step-wise decreases at 105 and 155 °C, that is, the T_gs of L-PS and PC, respectively. Furthermore,

the T_g of PC in PC/L-PS was not shifted by the addition of L-PS.

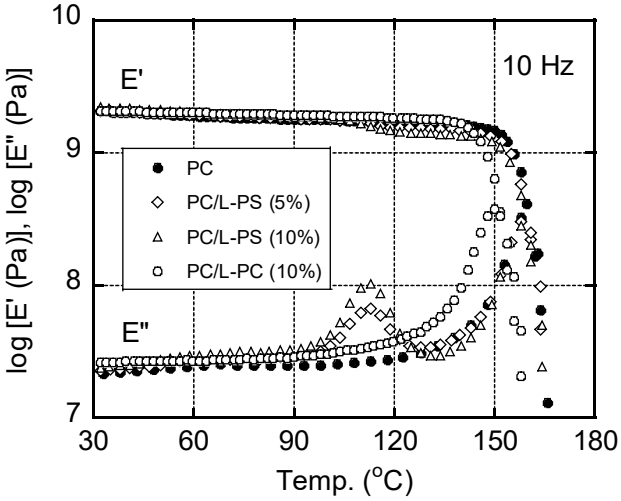

Figure 1 Temperature dependence of tensile storage modulus *E*' and loss modulus *E*" at 10 Hz for compression-molded films of PC, PC/L-PS (5%), PC/L-PS (10%), and PC/L-PC (10%)

This was reasonable because polystyrene is known to be immiscible with PC,[5-7] that is, the blends of PC/L-PS show a phase-separated structure. In contrast, a single T_g was detected for PC/L-PC, that is, a miscible blend, which was located at a temperature slightly lower than that of pure PC owing to the low molecular weight of L-PC.

Figure 2 shows the master curves of the frequency dependence of *G*' and *G*" in the molten state for PC, PC/L-PS (10%), and PC/L-PC (10%) at the reference temperature (T_r) of 250 °C. It was found that the time-temperature superposition principle was applicable even for PC/L-PS. The apparent flow activation energy was almost the same for all samples. Therefore, significant structure change, that is, phase-separation or phase-mixing, did not take place in this temperature range.

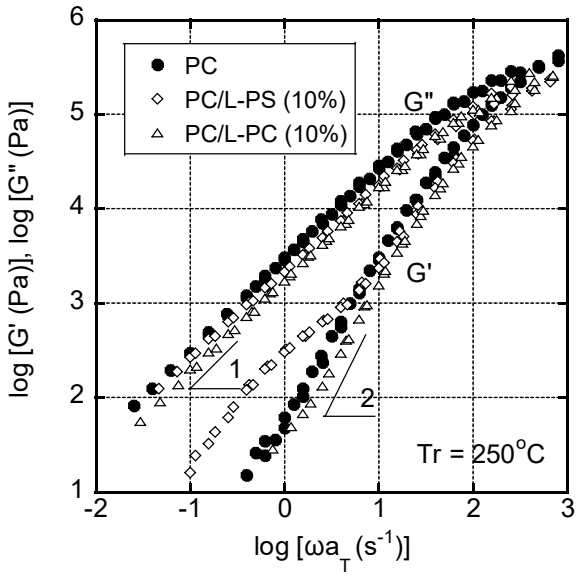

Figure 2 Master curves of frequency dependence of shear storage modulus *G*' and loss modulus *G*" at 250 °C for PC, PC/L-PS (10%), and PC/L-PC (10%)

Moreover, the *G*' values in the low frequency region for PC/L-PS were higher than those for PC. This is a well-known behavior for an immiscible blend having dispersions with lower modulus, which can be described by the emulsion model.[10,11] These results demonstrated that PC/L-PS has a phase-separated structure even in the molten state. In contrast, L-PC is, of course, miscible with PC, and the blend has a shorter relaxation time. Therefore, the *G*" values for PC/L-PC were lower than those for pure PC in the whole frequency range. The η_0 values, determined by $\lim_{\omega\to 0}\left(G''/\omega\right)$ at 250 °C for PC/L-PS (10%) and PC/L-PC (10%) were 2500 Pa s and 1800 Pa s, respectively. As compared with that of pure PC, i.e., 2800 Pa s, the addition of L-PS is not effective to decrease the zero-shear viscosity.

Although the linear viscoelastic properties suggest that L-PS does not have plasticization effect for PC, we observed a significant viscosity decrease from the capillary extrusion measurements. The flow curves of PC, PC/L-PS (5%), PC/L-PS

(10%), and PC/L-PC (10%) measured by the capillary rheometer with a circular die (L = 10 mm, D = 1 mm) at various temperatures are shown in Figure 3, in which the apparent values on the wall are plotted for both shear rate $\dot{\gamma}$ and steady-state shear viscosity η.

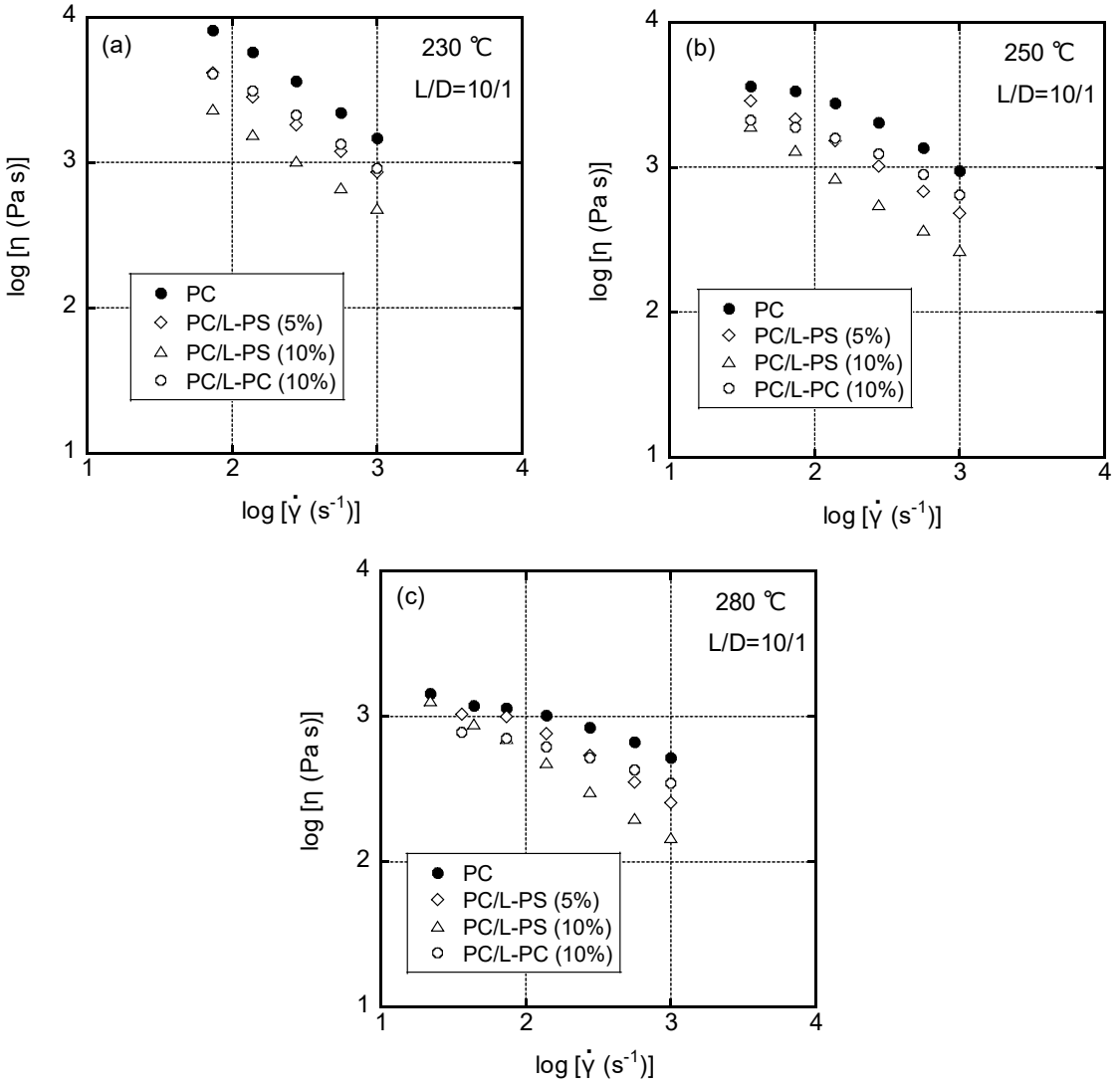

Figure 3 Flow curves at capillary extrusion for PC, PC/L-PS (5%), PC/L-PS (10%), and PC/L-PC (10%) at (a) 230 °C, (b) 250 °C, and (c) 280 °C

Figure 3 shows that the viscosity decreased with the L-PC addition in the wide

range of shear rates at all tested temperatures. This was a typical flow curve for plasticized polymer systems.[5,12)] However, the viscosity of PC surprisingly decreased with the addition of L-PS. Moreover, this viscosity decrease became significant in the high shear rate range, which did not correspond to the linear viscoelastic properties; i.e., The Cox-Merz rule is not applicable to the system.

Figure 4 shows the master curves of the shear stress measured by the capillary rheometer at 250 °C as a reference temperature. The shift factors were identical to those obtained by the master curve of the oscillatory shear modulus. PC/L-PS showed a similar shear stress level to PC in the low shear rate region, and a lower stress in the high shear rate region. Because the stress of PC/L-PC was lower than that of PC in the wide range of shear rates, the crossing behavior of the shear stress of PC/L-PS and PC/L-PC was detected around at 40 s^{-1}.

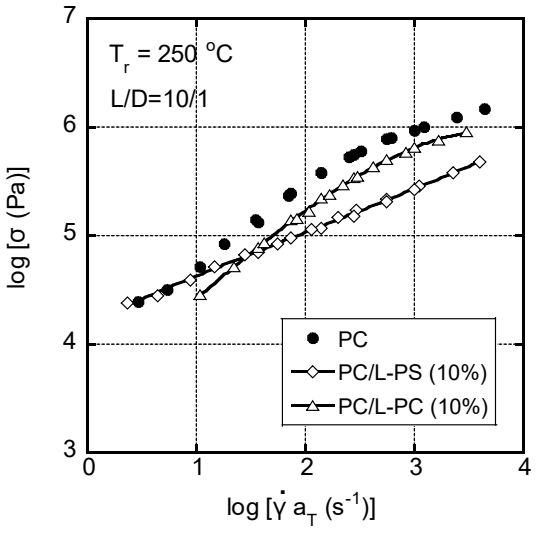

Figure 4 Master curves of apparent shear stress on wall σ
at 250 °C for PC, PC/L-PS (10%), and PC/L-PC (10%)

As a result of this viscosity decrease by the L-PS addition, the flowability at

injection-molding was enhanced. The spiral-flow length evaluated at 300 °C was greatly enhanced from 148 mm (pure PC) to 208 mm (PC/L-PS (5%)). This was reasonable because the viscosity decrease became significant especially in the high shear rate region.

At the capillary extrusion measurement, wall slippage can be the origin of an apparent viscosity decrease. The slippage behavior is known to be evaluated from the comparison of the shear stresses obtained using various dies having different die length L with the same length-to-diameter ratio L/D.[13-15)]

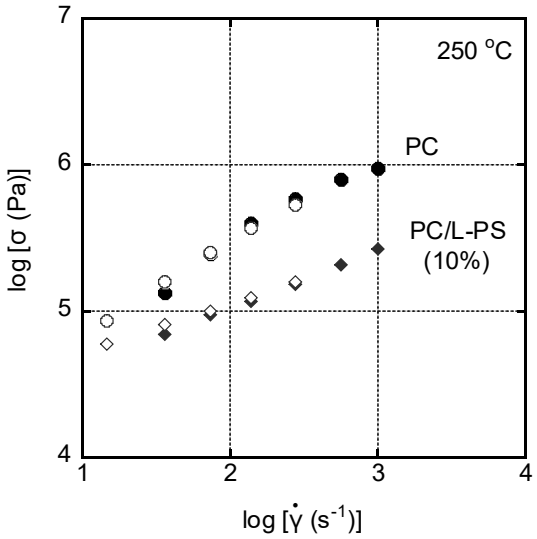

Figure 5 Apparent shear stress on wall σ at 250 °C for (circles) PC and (diamonds) PC/L-PS (10%) obtained by two capillary dies having the same L/D ratio.
(closed symbols) L/D=10/1 and (open symbols) L/D=20/2

Figure 5 shows the flow curves obtained using two dies with the same L/D ratio (10/1 and 20/2). When the slippage takes place, the apparent shear stress measured by a die with a smaller diameter is lower than that by a die with a large diameter. However, in the case of our measurement, the flow curves obtained from 10/1 and 20/2 were

identical, which demonstrated that the viscosity decrease was not attributed to the slippage on the wall. Furthermore, the extruded strands had a smooth surface without any distortion. Hence, flow instabilities, such as shark-skin originated from cohesive failure and/or adhesive failure on the wall surface and gross melt fracture owing to unsteady flow at the die entrance,[16-20] did not take place.

Figure 6 shows the Bagley plot, that is, pressure P versus the L/D ratio at various shear rates, for PC and PC/L-PS (90/10) at 250 °C. The intercept point of the vertical line (the pressure value at $L/D = 0$) indicates the pressure loss (P_e) at the entrance and end of a die. As shown in the figure, the end pressure correction was not required at least for PC except for the high shear rate 1000 s^{-1}, because P_e was almost zero in the wide range of shear rates (36 - 560 s^{-1}). Generally, the pressure loss becomes large for a polymer melt with high shear viscosity and/or high melt elasticity. In the present study, however, the values of the PC/L-PS having a lower viscosity were higher than those of the pure PC, which will be discussed in detail later.

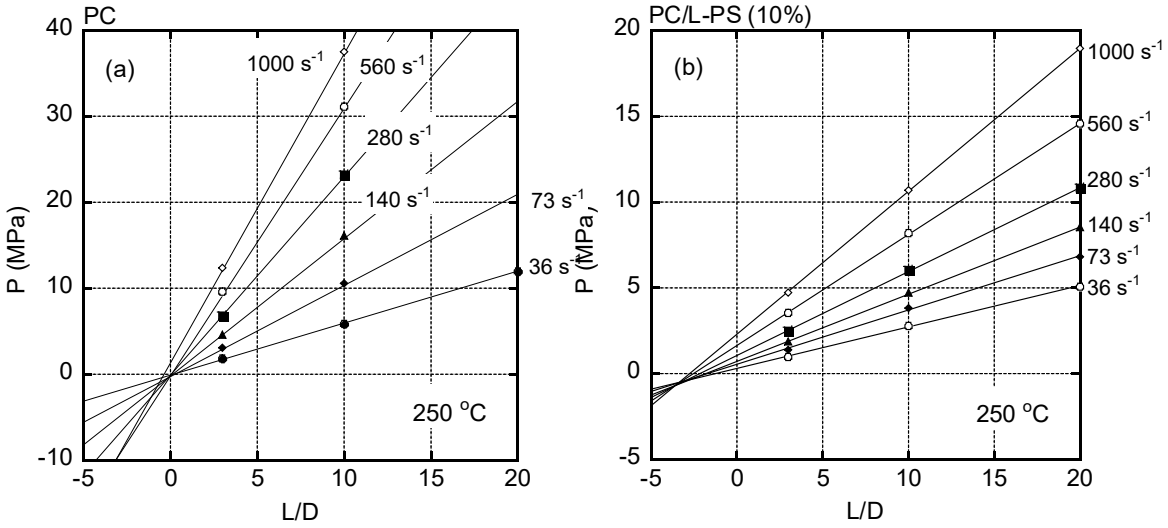

Figure 6 Bagley plots at 250 °C for (a) pure PC and (b) PC/L-PS (10%)

The viscosity decrease occurs not only under pressure flow but also drag flow. Figure 7 shows the growth curves of the shear viscosity at constant shear rates measured by the cone-and-plate rheometer. The oscillatory measurements were performed before/after the start-up flow to confirm that the edge part between the cone and plate was not scattered. At a shear rate of 0.1 s^{-1}, PC and PC/L-PS exhibited almost the same viscosity. However, at 2.3 s^{-1}, PC/L-PS showed an apparently lower viscosity than PC. Additionally, the time variation of viscosity for PC/L-PS had a declining trend, suggesting that the shear viscosity deviates from the value predicted by the linear viscoelastic properties. This indicated that the plasticization effect by L-PS proceeded gradually during the flow process, which demonstrated that both shear rate and residence time are important for this flow-induced viscosity-decrease phenomenon.

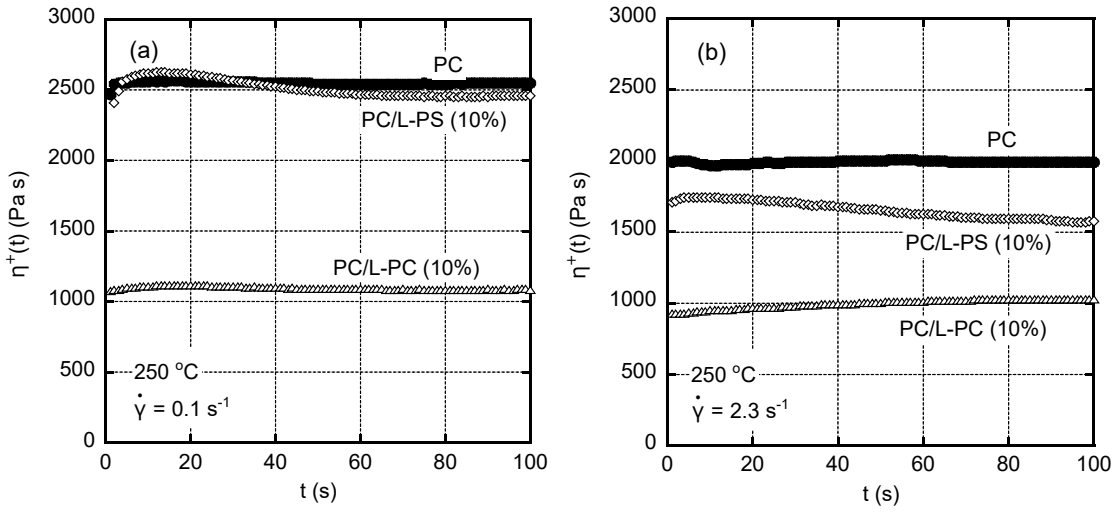

Figure 7 Growth curves of transient shear viscosity $\eta^+(t)$ at constant shear rates of (a) 0.1 $s^{-1}$and (b) 2.3 s^{-1} for PC, PC/L-PS (10%), and PC/L-PC (10%) measured by the cone-and-plate rheometer at 250 °C

Considering the results in Figure 6, the effect of the residence time in the capillary die on the shear viscosity must be responsible for the anomalous behavior of the end pressure decrease shown in Figure 6. Because the residence time increased with the die length, the pressure gradient P/L, which is proportional to the shear stress, decreased with L. As a result, the apparent slope in the Bagley plot became small, which provided a higher P_e for the PC/L-PS (10%) blend.

A segregation behavior of a low-molecular-weight fraction in a flow field has been reported for some polymer blend systems.[21,22] The localization of a low-molecular-weight fraction on the surface, if it occurs, leads to a large decrease in the apparent shear viscosity on the wall, although Figure 5 indicates that there was no obvious slippage on the surface. Therefore, we checked the concentration distribution in the cross-section of the extruded PC/L-PS strand cut along the flow direction using an FT-IR microscope. The peak intensity at 698 cm^{-1}, which was ascribed to the out-of-plane vibration of the C-H bonds in the phenyl ring in PS, and that at 887 cm^{-1}, which was ascribed to the stretching of the ester bond in PC, were used for the characterization. The peak intensity ratio was denoted as $A_{L\text{-}PS}/A_{PC}$. Figure 8 shows the distribution of the $A_{L\text{-}PS}/A_{PC}$ calculated from the IR absorption spectrum in the cross-section of a thin slice of the PC/L-PS (10%) strand extruded at 250 °C and 562 s^{-1}, which showed a large viscosity decrease.

The $A_{L\text{-}PS}/A_{PC}$ value was almost constant irrespective of the distance from the surface. Furthermore, the peak intensity at the surface of a strand, not a sliced sample, was measured directly by the ATR method and found to be identical to the $A_{L\text{-}PS}/A_{PC}$ value, that is, 0.60. Moreover, the value was independent of the apparent shear rate.

These results demonstrated that the segregation behavior of the L-PS fraction barely occurred during capillary extrusion.

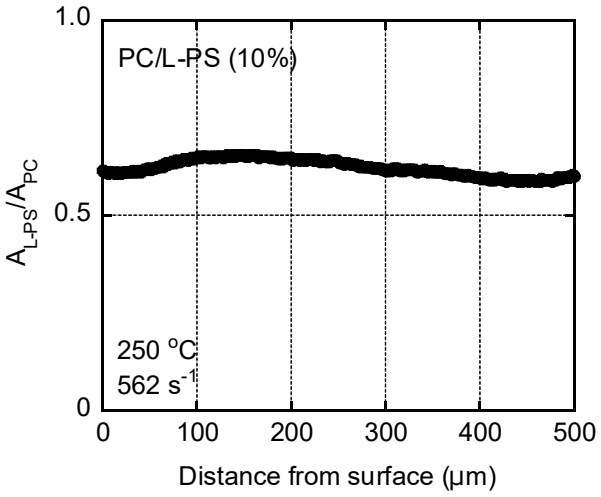

Figure 8 Distribution of $A_{\text{L-PS}}/A_{\text{PC}}$ in the cross-section of extruded PC/L-PS (10%, 250 °C, and 562 s^{-1}) strand

To discuss the origin of the viscosity decrease, the morphology of the extruded strands was observed using SEM. The morphology development of a polymer blend with sea-island structure, in which dispersions have lower viscosity, has been discussed in detail previously.[23-29] According to Taylor,[23] the morphology development in a blend of Newtonian liquids can be described by the capillary number (Ca) and viscosity ratio (λ).

$$Ca = \frac{\eta_m \dot{\gamma} r}{\Gamma} \tag{1}$$

$$\lambda = \frac{\eta_d}{\eta_m} \tag{2}$$

where η_m and η_d are the viscosities of the matrix and dispersion, respectively, r is the

radius of droplets, and Γ is the interfacial tension.

The capillary number can be understood as the ratio of the hydrodynamic stress required for the deformation of droplets to the interfacial stress that makes droplets in a spherical shape. When *Ca* is much larger than the critical value of the capillary number to show a break-up of droplets, that is, Ca_{crit}, the droplets will deform affinely to a great extent under both shear and elongational flow field.[27] Furthermore, the value of Ca_{crit} is known to be a function of λ and the type of flow. In particular, Ca_{crit} is low under elongational flow in a wide range of λ (even when $\eta_d << \eta_m$). Therefore, the dispersion with low viscosity can deform greatly under elongational flow, which occurs at the entry of a capillary die. Eventually, the deformed droplets show disintegration arising from the thermal fluctuation at the interphase, called Rayleigh disturbance, which is prominent after the cessation of flow. At the actual processing operation, the cooling process also plays a decisive role on the morphology. The surface region is quenched after extrusion, while the core is slowly cooled because a polymer at the surface will behave as a thermal insulator. As a result, the core region often has enough time to show a disintegration of deformed droplets, leading to satellites, i.e., small spherical droplets generated by the disintegration.[25,28]

Figure 9 shows the SEM images of the core and surface regions in the cross-section of the PC/L-PS (5%) strand extruded from a circular die with an *L*/*D* ratio of 10/1 (mm) at 250 °C and 562 s^{-1}. In the core region (Figure 9 (b)), deformed small particles align to the flow direction, which must be generated by the disintegration of deformed droplets arising from the Rayleigh disturbance. As mentioned before, dispersed droplets in the surface region should have more significant orientation than those in the core region

owing to its strong shear stress with prompt solidification. However, in the SEM image of the surface region (Figure 9 (a)), only spherical droplets were observed.

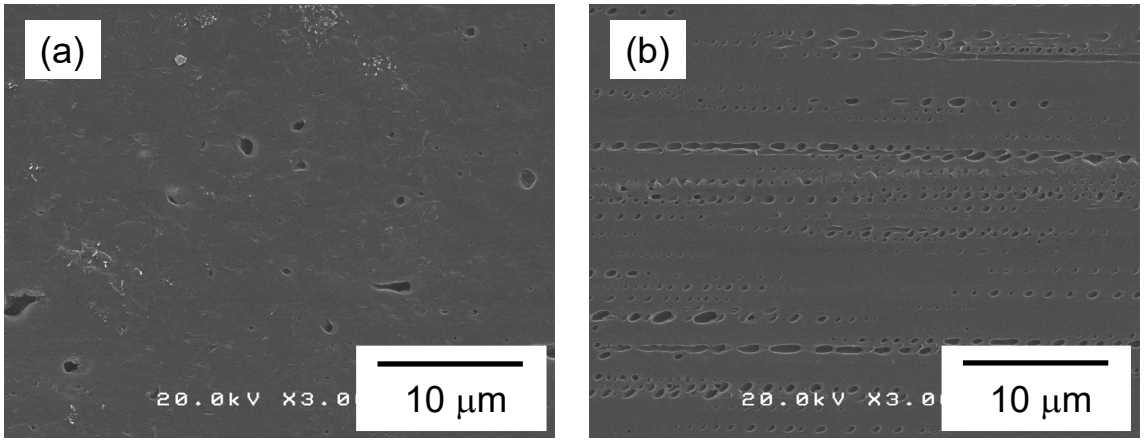

Figure 9 SEM images of (a) surface and (b) core regions in the cross-section for the PC/L-PS (5%) strand extruded from a die with L/D = 10/1 at 250 °C and 562 s^{-1}

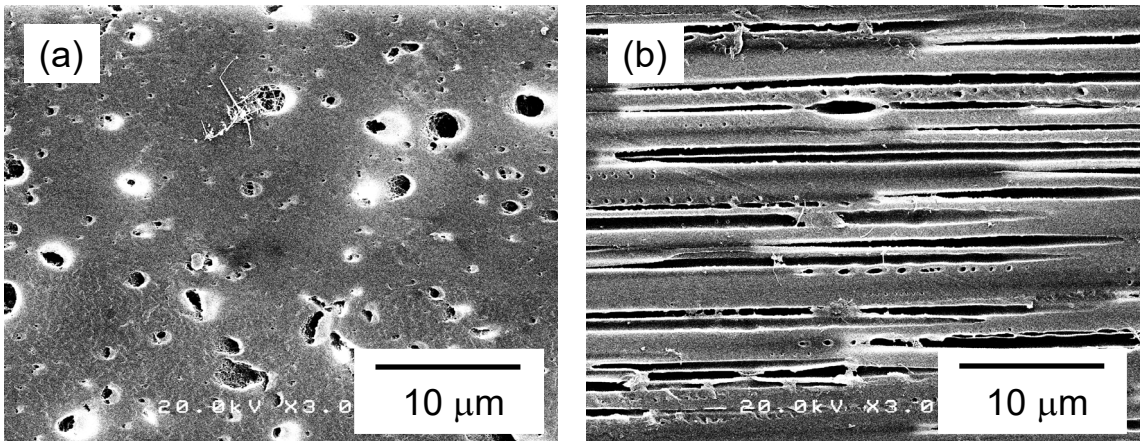

Figure 10 SEM images of (a) surface and (b) core regions in the cross-section for the PC/L-PS (10%) strand extruded from a die with L/D = 10/1 at 250 °C and 562 s^{-1}

A similar anomalous structure was detected in the PC/L-PS (10%) strand extruded at 250 °C and 562 s^{-1}, as shown in Figure 10. Moreover, the SEM images indicated that

the volume fraction of L-PS seemed to be higher in the core region.

These experimental results suggest that flow-induced phase-mixing occurred in the blend. It is known that the miscibility of a polymer blend can be affected by the flow field.[30-34] Flow-induced phase-mixing, which is attributed to the reduced concentration fluctuation[35] and/or the stored energy in polymer chains during flow,[36] has been reported for several polymer blend systems, such as PS/poly(vinyl methyl ether)[33] and poly(methyl methacrylate)/styrene-acrylonitrile co-polymers.[34] To the best of our knowledge, however, flow-induced phase-mixing has not been reported for PC/PS. Presumably, the contribution of mixing entropy would play an important role on the phenomenon, because we employed PS with low molecular weight. In the present system, L-PS became miscible with PC under a high shear stress in the capillary die and showed phase separation after cessation of flow, that is, extruded from the die exit. Then, the spherical L-PS droplets appeared near the surface when the solidification time was longer than the characteristic time required for phase separation. This may be the reason for the small volume fraction of the L-PS phase in the surface region. Moreover, the flow-induced miscibility would enhance the spiral-flow length owing to the T_g decrease by the dissolution of L-PS molecules.

Figure 11 shows the SEM image in the surface region of the cross-section for the PC/L-PS strand extruded at 250 °C and 562 s^{-1}, which was quenched by iced water immediately after the extrusion. In this experiment, the effect of the die length on the structure was also examined using two circular dies with L/D ratios of 10/1 and 3/1 (mm). The effect of quenching is obvious when Figure 11 (a) is compared with Figure 10 (a). In the case of the quenched sample (Figure 11 (a)), there were no or less spherical

droplets near the surface (ca. 15 μm from the surface), suggesting that the miscible state was frozen by the rapid solidification. Moreover, the strand having a short residence time in a capillary die (L/D = 3/1) was found to have more droplets. At the die entry, a large elongational strain, i.e., 4.6 as a Hencky strain, was applied. Because Ca must be much larger than Ca_{crit} under elongational flow even at $\lambda << 1$, the applied elongational stress deformed the droplets affinely irrespective of the die length. Consecutively, the shear strain was applied in the die land. Therefore, the structure difference in the figure indicates that the shear flow in the die land plays an important role on the phase-mixing.

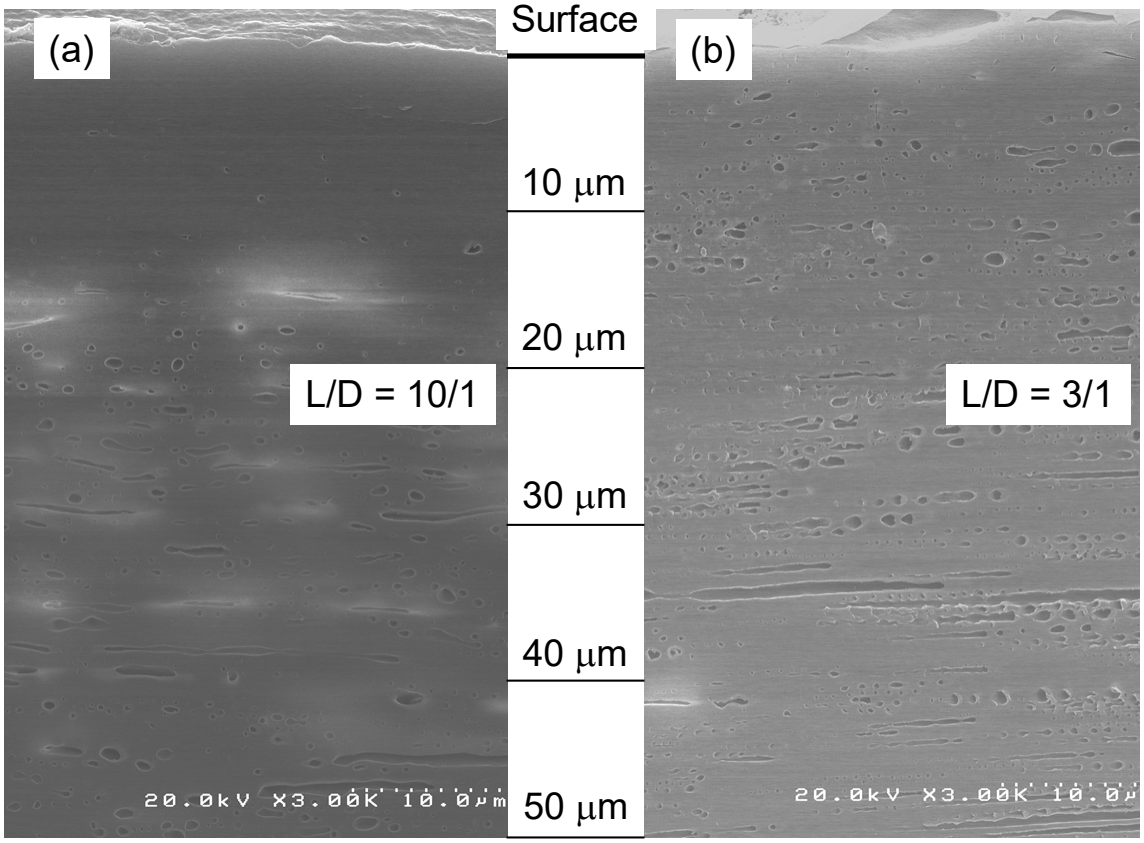

Figure 11 SEM images of the surface region in the cross-section for the PC/L-PS (10%) strand extruded from a circular die with L/D ratios of (a) 10/1 (mm) and (b) 3/1 (mm) at 250 °C and 562 s^{-1}. Both samples were quenched by iced water immediately

after extrusion. The depth from the surface was denoted in the figure.

Figure 12 shows the SEM image of the strand surface (not cross-section) for the PC/L-PS (90/10) extruded from a circular die with an *L*/*D* ratio of 10/1 at 250 °C and 562 s^{-1}. Although this strand was immersed into the solvent for etching, similar to the sliced samples, a dispersed droplet was not observed. Rapid cooling at the surface did not allow phase separation. This was another piece of evidence for the flow-induced phase-mixing.

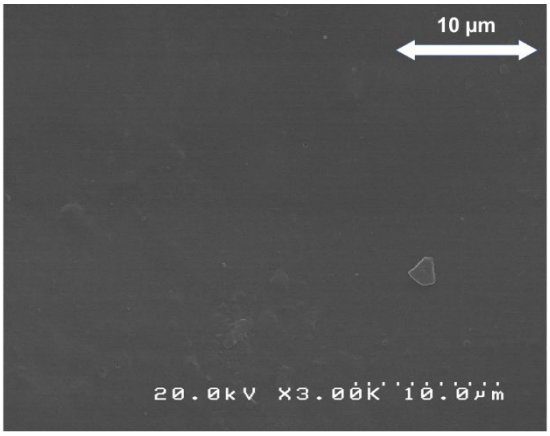

Figure 12 SEM image of the strand surface for PC/L-PS (10%) extruded from a die with *L*/*D* = 10/1 at 250 °C and 562 s^{-1}

However, the flow-induced phase-mixing cannot explain the mechanism for the large decrease in the shear viscosity because the viscosity of PC/L-PS was much lower than that of PC/L-PC, that is, the miscible blend. This viscosity decrease detected in this study could be affected by the fine and deformed dispersion of L-PS droplets in the fibrillar/layered structure, leading to slippage at the phase boundary and/or selective flow in the L-PS layer.

Although the exact mechanism of the viscosity drop is still unknown at present, we can demonstrate a new method to modify commercially available PC by the simple addition of L-PS. The blends show low shear viscosity with a great enhancement of flowability at injection-molding without losing transparency and heat resistance.

Conclusion

The rheological properties for binary blends composed of PC and L-PS were studied with the detailed characterization of structure in the strand extruded from a capillary rheometer. The binary blend of PC and L-PC was also employed as a reference sample. The L-PS addition greatly reduces the shear viscosity, which is more pronounced at high stress. The dispersed droplets in the extruded PC/L-PS blend are of a spherical shape in the surface area and are deformed greatly in the core. Furthermore, rapid cooling of the extruded strand reduces the number of droplets on the surface. These anomalous phenomena can be explained by the flow-induced phase-mixing under high stress condition. The large decrease in the shear viscosity, which leads to the enhanced spiral-flow length at injection-molding, could have a relation with the flow-induced phase-mixing.

Acknowledgement

A part of this work was supported by JSPS Grant-in-Aid for Scientific Research (B) Grant Number 16H04201 and Grant-in-Aid for JSPS Research Fellow Grant Number 18J12283.

References

[1] L. A. Utracki, Polymer alloys and blends; Thermodynamics and rheology, Hanser, Munich, 1990.

[2] W. M. Prest Jr., R. S. Porter, Rheological properties of poly(2,6-dimethylphenylene oxide) – polystyrene blends, J. Polym. Sci. Part A-2, Polym. Phys. 10 (1972) 1639-1655.

[3] A. Ajji, L. Choplin, R. E. Prud'Homme, Rheology of polystyrene/poly(vinyl methyl ether) blends near the phase transition, J. Polym. Sci. Part B, Polym. Phys. 29 (1991) 1573-1578.

[4] M. Yamaguchi, A. M. Mohd Edeerozey, K. Songsurang, S. Nobukawa, Material design of retardation films with extraordinary wavelength dispersion of orientation birefringence - A review, Cellulose 19 (2012) 601-613.

[5] C. Wisniewski, G. Marin, Ph. Monge, Viscoelastic behavior of non-compatible polymer blends: Polystyrene-polycarbonate, Eur. Polym. J. 21 (1985) 479-484.

[6] C. Z. Chuai, K. Almdal, I. Johannsen, J. Lyngaae-Jørgensen, Miscibility evolution of polycarbonate/polystyrene blends during compounding, Polym. Eng. Sci. 42 (2002) 961-968.

[7] W. N. Kim, C. M. Burns, Thermal behavior, morphology, and the determination of the Flory–Huggins interaction parameter of polycarbonate–polystyrene blends, J. Appl. Polym. Sci. 34 (1987) 945-967.

[8] W. Zhou, J. Osby, Siloxane modification of polycarbonate for superior flow and impact toughness, Polymer 51 (2010) 1990-1999.

[9] Y. Liang, X. Zhou, Y. Liao, J. Wu, X. Xie, H. Zhou, Reactive polycarbonate/diallyl

phthalate blends with high optical transparency, good flowability and high mechanical properties, Polymer 91 (2016) 89-97.

[10] J. E. Palierne, Linear rheology of viscoelastic emulsions with interfacial tension, Rheol. Acta 29 (1990) 204-214.

[11] M. Yamaguchi, H. Miyata, Influence of stereoregularity of polypropylene on miscibility with ethylene-1-hexene copolymer, Macromolecules 32 (1999) 5911-5916.

[12] T. Huang, M. Miura, S. Nobukawa, M. Yamaguchi, Crystallization behavior and dynamic mechanical properties of poly(L-lactic acid) with poly(ethylene glycol) terminated by benzoate, J. Polym. Environ. 22 (2014) 183-189.

[13] R. G. Larson, The structure and rheology of complex fluids, Oxford University Press, New York, 1988.

[14] C. W. Macosko, Rheology: Principles, measurements, and applications, Wiley, New York, 1994.

[15] S. Kotera, M. Yamaguchi, Capillary extrusion properties of ethylene-tetrafluoroethylene copolymer, J. Fluorine Chem. 176 (2015) 20-25.

[16] R. I. Tanner, Engineering rheology, Oxford Univ Press, New York, 1985.

[17] M. Yamaguchi, H. Miyata, V. Tan, C. G. Gogos, Relation between molecular structure and flow instability for ethylene/α-olefin copolymers, Polymer 43 (2002) 5249-5255.

[18] S. G. Hatzikiriakos, K. B. Migler, Polymer processing instabilities, CRC Press, Boca Raton, 2004.

[19] R. Koopmans, J. D. Doelder, J. Molenaar, Polymer melt fracture, CRC Press, Boca Raton, 2010.

[20] S. Q. Wang, Nonlinear polymer rheology: Macroscopic phenomenology and molecular foundation, Wiley, New York, 2018.

[21] F. Pisciotti, J. Lausmaa, A. Boldizar, M. Rigdahl, TOF-SIMS study of injection-molded polystyrene, Polym. Eng. Sci. 43 (2003) 1289-1297.

[22] T. Sako, A. Ito, M. Yamaguchi, Surface segregation during injection molding of polycarbonate/poly(methyl methacrylate) blend, J. Polym. Res. 24 (2017) 89.

[23] G. I. Taylor, The formation of emulsions in definable fields of flow, Proc. R. Soc. London A 146 (1934) 501-523.

[24] L. A. Utracki, Z. H. Shi, Development of polymer blend morphology during compounding in a twin-screw extruder. Part I: Droplet dispersion and coalescence – A review, Polym. Eng. Sci. 32 (1992) 1824-1833.

[25] M. Heindl, M. K. Sommer, H. Münstedt, Morphology development in polystyrene/polyethylene blends during uniaxial elongational flow, Rheol. Acta 44 (2004) 55-70.

[26] F. Oosterlinck, I. Vinckier, M. Mours, H. M. Laun, P. Moldenaers, Morphology development of a PS/PMMA polymer blend during flow in dies, Rheol. Acta 44 (2005) 631-643.

[27] H. E. H. Meijer, J. M. H. Janssen, P. D. Anderson, Mixing of immiscible liquids, in Mixing and compounding of polymers, theory and practice, in: I. Manas-Zloczower (Eds.), Mixing and Compounding of Polymers, 2nd ed., Hanser, Munich, 2009.

[28] M. Yamaguchi, K. Suzuki, H. Miyata, Structure and mechanical properties for binary blends of i-PP with ethylene-1-hexene copolymers, J. Polym. Sci. Part B

Polym. Phys. 37 (1999) 701-713.

[29] T. Yokohara, S. Nobukawa, M. Yamaguchi, Rheological properties of polymer composites with flexible fine fiber, J. Rheology 55 (2011) 1205-1218.

[30] H. W. Kammer, C. Kummerloewe, J. Kressler, J. P. Melior, Shear-induced phase changes in polymer blends, Polymer 32 (1991) 1488-1492.

[31] H. Yanase, P. Moldenaers, J. Mewis, V. Abetz, J. V. Egmond, G. G. Fuller, Structure and dynamics of a polymer solution subject to flow-induced phase separation, Rheol. Acta 30 (1991) 89-97.

[32] J. J. Magda, C. S. Lee, S. J. Muller, R. G. Larson, Rheology, flow instabilities, and shear-induced diffusion in polystyrene solutions, Macromolecules 26 (1993) 1696-1706.

[33] S. A. Madbouly, M. Ohmomo, T. Ougizawa, T. Inoue, Effect of the shear flow on the phase behaviour of polystyrene/poly(vinyl methyl ether) blend, Polymer 40 (1999) 1465-1472.

[34] S. A. Madbouly, T. Ougizawa, T. Inoue, Phase behavior under shear flow in PMMA/SAN blends: Effects of molecular weight and viscosity, Macromolecules 32 (1999) 5631-5636.

[35] T. Ougisawa, T. Inoue, Morphology of polymer blends, in L. A. Utracki, C. A. Wilkie (Eds.), Polymer blends handbook, 2nd ed., Hanser, Munich, 2014.

[36] W. Soontaranun, J. S. Higgins, T. D. Papathanasiou, Fluid Phase Equilibria, 121 (1996) 273-292.